Bioorganic & Medicinal Chemistry 20 (2012) 2897–2904

Contents lists available at SciVerse ScienceDirect

Bioorganic & Medicinal Chemistry

journal homepage: www.elsevier.com/locate/bmc

Syntheses of [12]aneN$_3$–oligopeptide conjugates as effective DNA condensation agents

Zhi-Fen Li [a], Zhi-Fo Guo [a], Hao Yan [a], Zhong-Lin Lu [a,*], Da-Yong Wu [b,*]

[a] College of Chemistry, Beijing Normal University, Beijing 100875, China
[b] Key Laboratory of Photochemical Conversion and Optoelectronic Materials, TIPC, CAS, Beijing, China

ARTICLE INFO

Article history:
Received 20 January 2012
Revised 7 March 2012
Accepted 8 March 2012
Available online 24 March 2012

Keywords:
[12]aneN$_3$
Oligopeptide
DNA condensation
Gel-electrophoresis
Atomic force microscopy

ABSTRACT

With the aim to develop effective and low toxicity DNA condensation agents, a series of oligopeptide derived macrocyclic polyamine [12]aneN$_3$ conjugates **7a**–**h**·3HCl have been designed and synthesized through multi-step amidation reactions. Structure–property study through gel electrophoresis proved that the conjugates containing high hydrophobic ending amino acids exhibited effective condensation ability at concentration of 150–250 μM, which was further confirmed by dynamic light scattering and atomic force microscopy experiments. EB displacement assay, ionic salt effect, and structure–property relationship in gel electrophoresis indicated that DNA condensation resulted from both the electrostatic interaction of [12]aneN$_3$ unit and hydrogen-bonding/hydrophobic multi-interaction of oligopeptide moiety in the conjugates with DNA. The reversible condensation process and their low cytotoxicity suggest that the new condensing agents are potential for the development of non-viral vectors.

1. Introduction

Gene therapy has attracted intensive attention as a promising method for treating both congenital and acquired diseases such as cancer, AIDS, Parkinson's and Alzheimer's diseases, arthritis, and heart diseases. The challenge of successful gene therapy relies heavily on the development of effective and safe carrier vectors capable of compacting and delivering DNA. Viral vectors are the preferred system in clinical trials due to their high efficiency, but their cytotoxicity, mutagenesis, carcinogenesis, and immune response limit their wide use. To this end, rapid advances have recently been made in the design and syntheses of non-viral gene vectors due to their advantages including adjustable structure, non-immunogenicity, and potential for large-scale production over viral vectors.[1–4] Non-viral gene vectors reported so far include multivalent cations derived from small organic molecules such as spermine and spermidine,[5] as well as organic polymers such as polyamines,[6,7] polysaccharides,[8] cationic lipids,[9–11] polypeptides,[12–14] dendrimers[15] and metal complexes.[16–20] Macrocylic polyamines such as [9]aneN$_3$, [12]aneN$_3$, and [12]aneN$_4$, which has multiple nitrogen atoms and unfolded conformations and can serve as suitable cationic units to interact with negative charged phosphate in the DNA backbone and induce desired condensation, they have been incorporated in cationic lipids and organic polymers and proved their applicability as DNA condensation agents and non-viral gene vectors more recently.[21–23] In spite of the various non-viral vectors that have been investigated, small organic molecules capable of effectively condensing DNA remain largely undeveloped, especially when considering the effective concentration and toxicity.

In this paper, we report herein on the preparation of a series of oligopeptide derived macrocyclic polyamine conjugates (see Scheme 1) and their capabilities of inducing DNA condensation. By varying the structure of ending amino acid in the oligopeptide moieties, structure–activity relationship of these compounds has been examined by using gel electrophoresis, dynamic light scattering, and atomic force microscopy. The obtained data clearly demonstrates that the conjugates containing more hydrophobic side chains are highly efficient in condensing plasmid DNA into particulate structures and with lower toxicity.

2. Results and discussion

2.1. Preparation of [12]aneN$_3$–oligopeptides

Studies on mechanism of DNA condensation indicate that major factors responsible for effective condensation include electrostatic force, groove binding, and/or intercalation. The structure of the designed conjugates is similar to cationic liposome. It is anticipated that the macrocyclic polyamine [12]aneN$_3$ moiety will act as cationic unit responsible for electrostatic interaction, while the oligopeptide unit will act as hydrophobic moiety in cationic liposome to make multiple interaction with DNA and enhance the condensation process. At the same time, the incorporation of oligo-

* Corresponding authors. Tel./fax: +86 10 58801804.
E-mail addresses: luzl@bnu.edu.cn (Z.-L. Lu), dayongwu@mail.ipc.ac.cn (D.-Y. Wu).

0968-0896/$ - see front matter © 2012 Elsevier Ltd. All rights reserved.
http://dx.doi.org/10.1016/j.bmc.2012.03.022

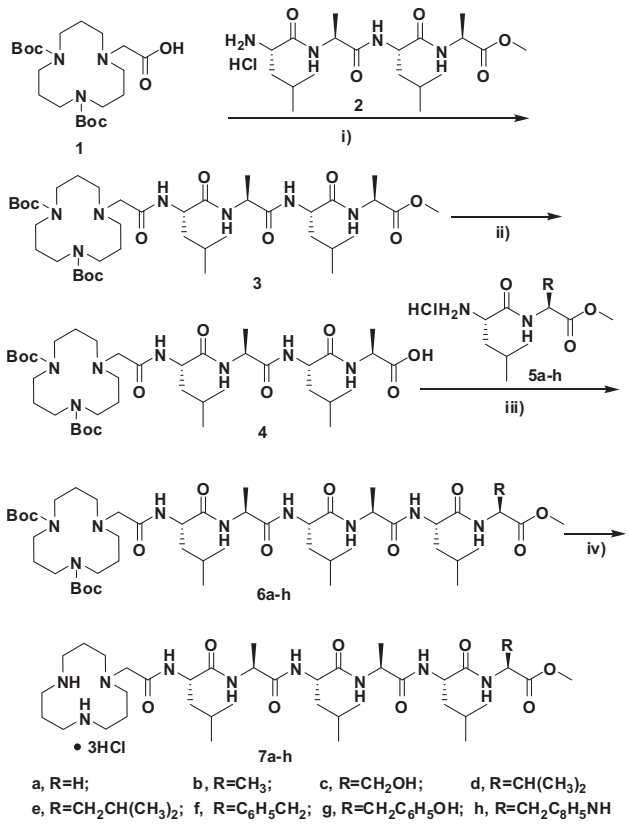

Scheme 1. Synthesis of [12]aneN$_3$–CH$_2$CO–hexapeptide conjugates **7a**–**h**. Reagents: (i) HATU, DIEA, CH_2Cl_2; (ii) LiOH·H_2O, MeOH, H_2O; (iii) HATU, DIEA, DMF; (iv) MeOH/HCl.

peptides is expected to reduce the toxicity of the conjugates due to their biocompatibility. Furthermore, the hydrophobic properties of the oligopeptide moieties were varied by using different terminal amino acid to study the structure–activity relationship.

All the peptides used in the study were synthesized by liquid phase procedure. The synthetic route to the conjugates **7a**–**h** is shown in Scheme 1. Compound **1** was first prepared, which was coupled with tetrapeptide **2** to give product **3**. Later hydrolysis of compound **3** by LiOH resulted in acid **4**. The acid **4** was coupled with a series of H_2N-dipeptides 5**a**–**h** in the presence of HATU to afford compounds **6a**–**h**. The target conjugates **7a**–**h** were obtained by N-Boc deprotection (4 M HCl in methanol) of **6a**–**h**. The yields of the last two steps were about 40–60%. All new compounds were characterized by ^{1}H NMR, ^{13}C NMR, IR, ESI-MS, or HR-MS (see Supplementary data).

2.2. Retardation of gel electrophoresis

The ability of each conjugates to condense a plasmid DNA was evaluated by gel electrophoresis assay. As shown in Figure 1, as the concentration of the conjugates **7a**–**h** increased, the amount of supercoiled DNA gradually diminished. For conjugates **7a**–**c**, **7d** and **7g**, complete retardation of electrophoresis was not observed even when the concentration reached to 500 μM. For conjugates **7e**, **7f**, and **7h**, the migration of DNA are completely retarded at 200, 250, and 250 μM, respectively.

At pH 7.4, all the plasmid DNA phosphate functions are negatively charged, and the [12]aneN$_3$ unit in the conjugates **7a–h** are positively charged. The decrease of the mobility of plasmid DNA as the increase of the conjugate concentrations is mainly due to the charge neutralization. However, the different performance of each conjugates clearly indicates that the electrostatic effects from macrocyclic polyamines is one aspect in the DNA condensation process, the interaction between the oligopeptides and DNA also contributes to the process. From the above results, it clearly demonstrates that the hydrophobicity of the terminal amino acids in hexapeptides side chain plays an important role for the DNA condensation process.[24] It can be seen that the efficient DNA condensations were achieved with the terminal amino acids with higher hydrophobic index (HI), such as leusine (HI = 1.1) in **7e**, phenylalanine (HI = 1.2) in **7f**, and tryptophan (HI = 0.81) in **7h**; while poor or no DNA condensation were found for the terminal amino acids with lower hydrophobic index, such as tyrosine (HI = 0.26) in **7g** and serine (HI = −0.18) in **7c** even at 500 μM.[25] Thus conjugates **7e**, **7f**, and **7h** were studied in more detail in the following work.

2.3. Dynamic light scattering

Dynamic light scattering (DLS) is a powerful tool for measuring particle size distributions (PSDs) in solution.[26] Here, DLS technique was used to investigate the DNA condensation in solutions in the presence of different concentrations of **7e**, **7f**, and **7h**, respectively. As shown in Figure 2, the measurements were performed at DNA concentration of 9 μg/mL in Tris–HCl buffer (50 mM, pH 7.4) at 25 °C. The obtained results revealed that the hydrodynamic diameters of DNA particles condensed by **7e**, **7f**, and **7h** were ranging from 174 to 318 nm, 208 to 365 nm, 196 to 563 nm, respectively. The results are consistent with examples reported in literatures that the sizes of the DNA nano-particles increased with the increase of the concentrations of condensing agents.[16] To be noticed, there should be a saturation in the particle size at higher concentration of the conjugates.[18]

2.4. Atomic force microscopy

Additional evidence supporting DNA condensation was provided by atomic force microscopy (AFM).[16] Figure 3 shows the typical AFM images of pUC18 in the absence and presence of **7e**, **7f**, and **7h** at the concentration to induce complete condensation. AFM image in the absence of the conjugates showed that naked DNA formed closed loops displaying twists of its strands (Fig. 3a).[27] Upon the addition of 150 μM of **7e**, the DNA molecules were induced to form nanoparticles with a diameter of 30–294 nm (Fig. 3b), The diameters of the DNA nanoparticles condensed by **7f** and **7h** at concentrations of 250 μM were 20–69 and 36–214 nm, respectively (Fig. 3c and d). The AFM images clearly demonstrate the effective DNA condensation ability of **7e**, **7f**, and **7h**. The particle sizes revealed by AFM were smaller than DLS as literature reported, which is can be attributed to the different sampling techniques used in these two experiments.[28]

2.5. EB displacement assay

Ethidium bromide (EB) displacement assays were conveniently used to assess the binding ability of compound **7e**, **7f**, and **7h** with DNA. EB has weak fluorescence, its fluorescence is greatly enhanced when intercalating with DNA. It is known that this enhanced fluorescence can be reduced or quenched by the addition of other compounds having the ability to bind to DNA, which can be used to evaluate the binding ability of other molecules. As shown in Figure 4, the fluorescence intensity of EB-bound CT-DNA was reduced upon the addition of conjugates **7e**, **7f**, and **7h**. The apparent binding constants (K_{app}) were calculated to be $(1.9 \pm 0.2) \times 10^5\ M^{-1}$, $(1.4 \pm 0.1) \times 10^5\ M^{-1}$, and $(1.2 \pm 0.1) \times 10^5\ M^{-1}$ for **7e**, **7f**, and **7h**, respectively. These binding constants are close to those of the bifunctional compounds containing two [12]aneN$_3$ moieties, which

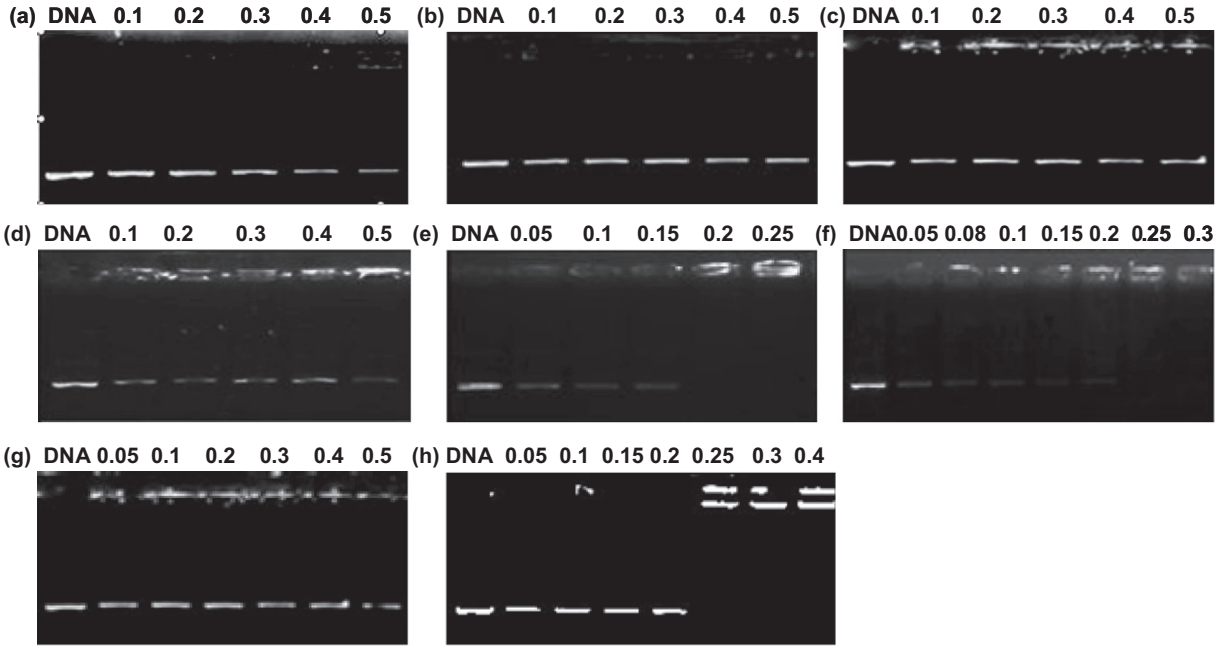

Figure 1. Agarose gel electrophoresis assay to investigate the pUC18 DNA condensation in the presence of [12]aneN$_3$–CH$_2$CO–hexapeptide conjugates **7a** (a), **7b** (b), **7c** (c), **7d** (d), **7e** (e), **7f** (f), **7g** (g), and **7h** (h) at different concentrations in Tris–HCl buffer (50 mM, pH 7.4, and 37 °C). The values shown on the figures are concentrations (mM) of the conjugates. The most left lane in each figure indicates the mobility of DNA alone in the gel.

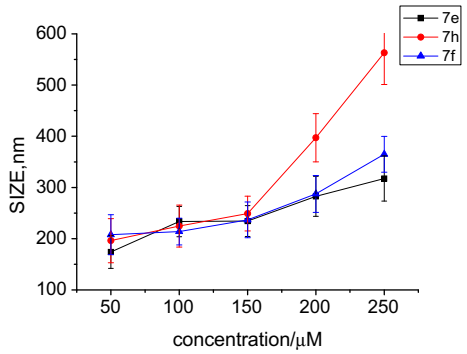

Figure 2. Hydrodynamic diameter distributions of pUC18 DNA particles condensed by **7e**, **7f**, and **7h** at concentrations of 50, 100, 150, 200, 250 μM, respectively. Scattering angle of 90° at 25 °C. The DNA concentration is 9 μg /mL. Values expressed as mean ± S.D. $n = 10$.

clearly indicates that oligopeptide moieties in **7e**, **7f**, and **7h** facilitate the interaction between the conjugates and the plasmid DNA.

2.6. Ionic strength effect

To evaluate the contribution of the electrostatic effect in the DNA condensation induced by **7e**, **7f**, and **7h**, the effect of ionic strength in buffer solutions was examined. As shown in Figure 5, the amount of uncondensed supercoiled DNA increased along the increase of NaCl concentrations from 0 to 400 mM, which obviously implies that the condensing agents bind largely with the anionic phosphate in DNA via electrostatic interactions. Addition of excess salt partially neutralizes the phosphate backbone, which in turn decrease the binding of the conjugates with DNA.[29,30]

2.7. Release of the compact DNA

The release process of DNA condensates plays a crucial role in determining the effectiveness of the condensates to deliver the therapeutic gene into the target cell nucleus. Several experiments have been applied to modulate the DNA dissociation from the condensates, such as pH jump,[31] linkage break,[32] and temperature.[33] In this work, high concentration of NaCl solution was used to evaluate the reversibility of DNA condensation. As shown in Figure 6, it is obvious that the condensed DNA could be partially released after being treated with 200 mM of NaCl, this clearly indicates that the DNA condensation induced by **7e**, **7f**, and **7h** was reversible. On the other hand, there are still large amount of the condensates kept in the loading well, which showed their stability of the condensates, especially at the lower concentration of NaCl.

2.8. Cytotoxicity assay

As potential gene vectors, the condensing agents are desired to have low toxic effect on cells. Hence the cytotoxicity profiles for **7e**, **7f**, and **7h** were evaluated by the MTT assay against T98G and HepG2 cell lines.[26] As shown in Figure 7, three compounds did not exhibit obvious cytotoxicity towards T98G and HepG2. At the concentration of 250 μM for the conjugates **7e**, **7f**, and **7h**, the viabilities of T98G were 96%, 78% and 80%, and those of HepG2 were 97%, 83% and 85%, respectively. It can be seen that the toxicity of oligopeptide derived macrocyclic polyamines are less than those of the bifunctional condensing agents we developed in the previous work.[27] The incorporation of oligopeptide unit into macrocyclic ploy amines really benefits their biocompatibility. Lower toxicity of the three conjugates provides the possibility for the development of non-viral gene vector.

3. Conclusion

In this study, a series of [12]aneN$_3$–CH$_2$CO–hexapeptide conjugates were designed, synthesized, and fully characterized. Their capabilities in condensing DNA were studied with gel electrophoresis, fluorescence spectra, dynamic light scattering, and atomic force microscopy techniques. It proved that the high hydrophobic property of the oligopeptides unit in the conjugates favors the DNA condensation process. The condensation of plasmid DNA can be

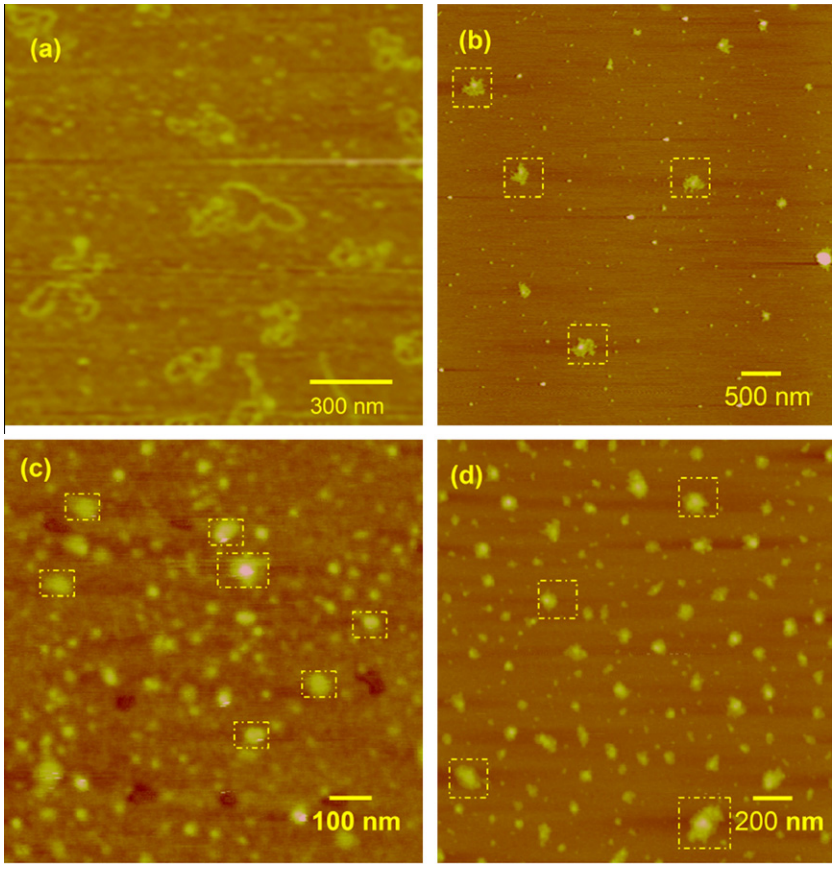

Figure 3. AFM Images of pUC18 DNA (9 μg/mL) and its condensation induced by the conjugates: (a) DNA (b) DNA + 150 μM **7e**; (c) DNA + 250 μM **7f**. (d) DNA + 250 μM **7h**.

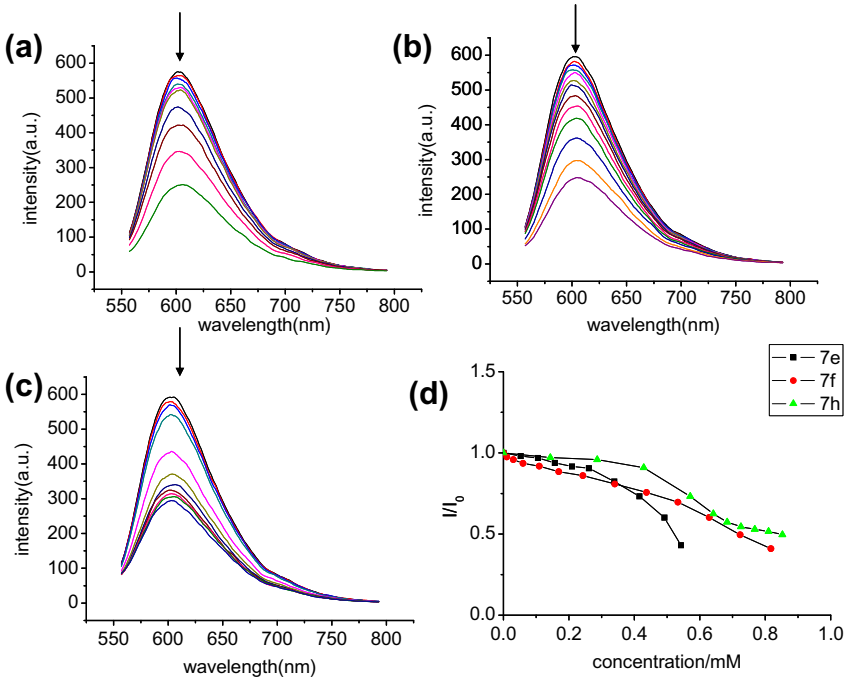

Figure 4. Fluorescence quenching curves of EB bound ct-DNA by **7e**, **7f**, and **7h** in 5 mM Tris–HCl/50 mM NaCl solution, pH 7.4, λ_{ex} = 537 nm, [EB] = 4 μM, DNA = 40 μM, [conjugate] = 0–0.9 mM, 25 °C. The arrow shows the intensity changes on increasing concentration of **7e** (a), **7f** (b), and **7h** (c).

occurred at 150 μM of the conjugate, 37 °C and pH 7.4, and the process is partially reversible in the presence of higher concentration (200 mM) NaCl. The effective DNA condensation ability of the conjugates **7e**, **7f**, and **7h** can be attributed to the electrostatic effect

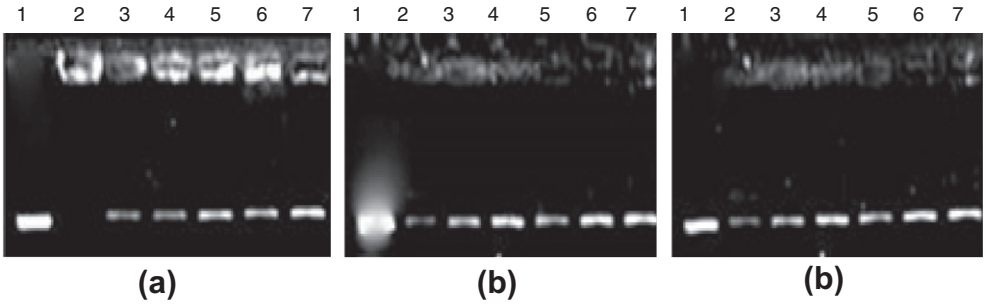

Figure 5. Agarose gel electrophoresis assay to investigate the effect of ionic strength of DNA condensation by 150 μM **7e** (a), 150 μM **7f** (b) and 220 μM **7h** (c) in Tris–HCl buffer (50 mM, pH 7.4), [DNA] = 9 μg/mL. Lane 1, DNA control; Lane 2–7, [NaCl] = 0, 50, 100, 200, 300, 400 mM.

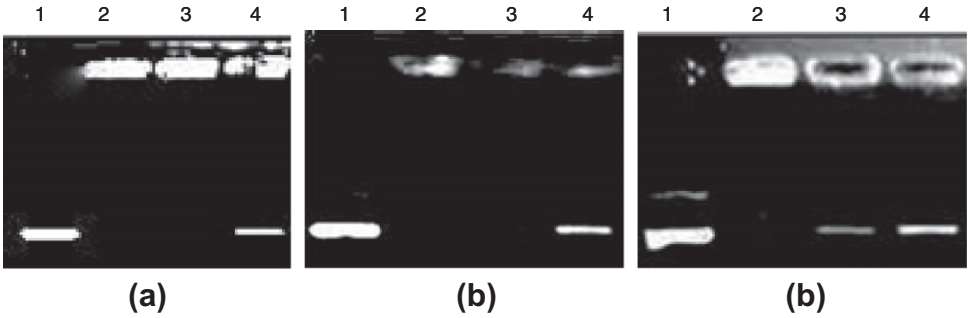

Figure 6. Agarose gel electrophoresis assay to investigate the reversibility of DNA condensation in Tris–HCl buffer (50 mM, pH 7.4): (a) DNA + 150 μM **7e** + NaCl; (b) DNA + 250 μM **7f** + NaCl; (c) DNA + 250 μM **7h** + NaCl. Lane 1, DNA control, lane 2–4, [NaCl] = 0, 100, 200 mM.

resulted from the positive charged [12]aneN_3 moiety and the hydrogen bonding and hydrophobic multi-interactions from oligopeptide unit in the conjugates. For **7h**, aromatic–aromatic interaction should also be a potential contributor. The lower cytotoxicity of the three [12]aneN_3–oligopeptide condensing agents make them desirable for the development of non-viral gene vectors. Further investigations are still undergoing in this lab.

4. Experimental section

4.1. Materials and methods

All chemicals and reagents were obtained commercially and used without further purification. All amino acid, HATU and DIEA were obtained commercially from Beijing Ou He Company (China). Calf thymus DNA (CT-DNA) and plasmid DNA (pUC18) were purchased from Solarbio Company (China). The concentrations of CT-DNA were determined by UV spectroscopy at 260 nm, taking 6600 M^{-1} cm^{-1} as the molar absorption coefficient. All solvents and reagents were of analytical grade and were used as received. Ultrapure milli-Q water (18.25 MΩ) was used in all DNA condensation assays.

^{1}H NMR and ^{13}C NMR spectra were obtained on a Bruker Avance III 400 MHz spectrometer at 25 °C. Chemical shifts were referenced on residual solvents peaks. ESI-MS and HRMS were acquired on a Waters Quattro Mocro spectrometer and Bruker Daltonics Bio TOF mass spectrometer, respectively. IR spectra were taken on a Nicolet 380 spectrometer. Fluorescence spectra were recorded on a Varian Cary Eclipse Spectrometer. All experiments were performed in Tris buffer (5 mM Tris–HCl/50 mM NaCl, pH 7.4) at room temperature. Hydrodynamic diameters (DLS) were determined using a DynaPro Nanostar dynamic laser light scattering apparatus. Atomic force microscopy (AFM) images were obtained with a Veeco NanoScope IIIa atomic force microscope. UV/Vis spectra were measured on a Varian Cary 300 UV/Vis spectrophotometer using solutions in 1.0 cm quartz cuvettes.

4.2. Synthesis

Details for the preparation and characterization of compounds **1**, **2**, **3**, **4**, **5a**–**h**, and **6a–h** can be found in the Supplementary data. A typical procedure for the preparation of compounds **7a–h**·3HCl was described as follows.

Acetyl chloride (14.0 g, 178 mmol) dissolved in methanol (30 mL) at ice bath, then the Boc-protected compound **6a–h** was added. The mixture was stirred at room temperature for 12 h. The solvent was removed at reduced pressure and the remaining solid was washed with chloroform and dried in vacuum to give **7a–h**·3HCl.

4.2.1. [12]aneN_3–CH_2COLeuAlaLeuAlaLeuGlyOCH$_3$·3HCl, 7a·3HCl

Yield, 81%. ^{1}H NMR (400 MHz, DMSO+D_2O) δ (ppm) 4.35–4.22 (m, 5H), 3.88–3.72 (m, 2H), 3.60 (s, 3H), 3.52 (s, 2H), 3.15–3.04 (m, 12H), 2.02 (s, br, 2H), 1.86 (s, br,4H), 1.58 (s, br, 4H), 1.50–1.39 (m, 5H), 1.19 (t, J = 6.9 Hz, 6H), 0.89–0.81 (m, 18H). ^{13}C NMR (101 MHz, DMSO) δ (ppm) 172.3, 171.8, 171.6, 171.5, 171.1, 170.0, 54.7, 51.6, 51.3, 50.8, 50.7, 48.0, 41.0, 40.8, 40.6, 40.4, 24.1, 24.0, 23.9, 23.0, 22.9, 21.5, 21.4, 17.8, 17.7. IR (KBr, cm^{-1}): 3435, 3274, 2957, 1736, 1633, 1548, 1443, 1383, 1365, 1212, 1161. HRMS-ESI: m/z Calcd for $C_{38}H_{72}N_9O_8$ $[M+H]^+$ 782.5504, Found: 782.5516.

4.2.2. [12]aneN_3–CH_2COLeuAlaLeuAlaLeuAlaOCH$_3$·3HCl 7b·3HCl

Yield, 88%. ^{1}H NMR (400 MHz, DMSO+D_2O) δ (ppm) 4.35–4.21(m, 6H), 3.59 (s, 3H), 3.53 (s, 2H), 3.13–3.03 (m, 12H), 2.02 (s, br, 2H), 1.83 (s, br,4H), 1.61–1.55 (m, 3H), 1.50–1.41 (m, 6H), 1.33–1.16 (m, 9H), 0.92–0.80 (m, 18H).^{13}C NMR (101 MHz, DMSO) δ (ppm) 172.9, 172.0, 171.9, 171.7, 171.3, 54.7, 51.9, 51.4, 51.0, 50.7, 48.2, 47.5, 40.9, 40.7, 40.6, 24.2, 24.1, 24.0, 23.1, 21.6, 21.4, 17.9, 17.7, 16.8. IR (KBr, cm^{-1}): 3436, 3270, 3078, 2957, 1736, 1632, 1548, 1452, 1383, 1368, 1218, 1158.HRMS-ESI: m/z Calcd for $C_{39}H_{74}N_9O_8$ $[M+H]^+$ 796.5660, found: 796.5666.

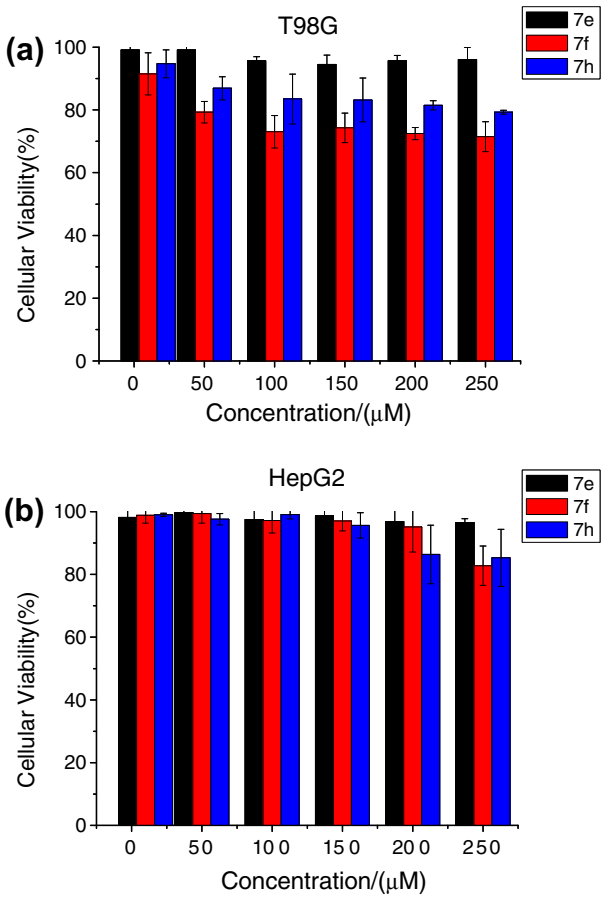

Figure 7. Relative viabilities of T98G and HepG2 cells in the presence of different concentrations of **7e**, **7f**, and **7h** after incubation at 37 °C for 24 h. Each point represents the means of three experiments.

4.2.3. [12]aneN$_3$–CH$_2$COLeuAlaLeuAlaLeuSerOCH$_3$·3HCl 7c·3HCl

Yield, 80%. ^{1}H NMR (400 MHz, DMSO+D$_2$O) δ (ppm) 4.35–4.21 (m, 6H), 3.75–3.67 (m, 2H), 3.62–3.60 (s, 5H), 3.15–3.04 (m, 12H), 2.03 (s, br, 2H), 1.85 (s, br, 4H), 1.62–1.54 (m, 3H), 1.48–1.39 (m, 6H), 1.19 (t, J = 6.5 Hz, 6H), 0.89–0.80 (m, 18H). ^{13}C NMR (101 MHz, DMSO) δ (ppm) 172.0, 171.9, 171.6, 171.5, 171.2, 170.8, 61.1, 54.8, 54.7, 51.7, 51.3, 51.2, 50.9, 50.7, 48.5, 48.0, 40.9, 40.8, 40.6, 24.2, 24.0, 23.1, 21.5, 21.4, 17.9, 17.7. IR (KBr, cm^{-1}): 3430, 3270, 2956. 2871, 1733, 1693, 1630, 1545, 1454, 1380, 1365, 1233, 1155. HRMS-ESI: m/z Calcd for $C_{39}H_{74}N_9O_9$ [M+H]$^+$ 812.5610; found: 812.5609.

4.2.4. [12]aneN$_3$–CH$_2$COLeuAlaLeuAlaLeuValOCH$_3$·3HCl 7d·3HCl

Yield, 88%. ^{1}H NMR (400 MHz, DMSO+D$_2$O) δ (ppm) 4.37–4.23 (m, 5H), 4.16–4.12 (m, 1H), 3.61 (s, 3H), 3.44 (s, 2H), 3.15–3.03 (m, 12H), 2.05–2.00 (m, 3H), 1.84 (s, br,4H), 1.62–1.53 (m, 4H), 1.48–1.39 (m, 5H), 1.33–1.16 (m, 6H), 0.94–0.81 (m, 24H). ^{13}C NMR (101 MHz, DMSO) δ (ppm) 172.2, 171.9, 171.7, 171.5, 171.3, 57.3, 55.0, 51.7, 51.2, 50.9, 50.0, 40.8, 40.7, 40.6, 29.9, 24.2, 24.0, 23.0, 21.6, 21.5, 21.4, 18.9, 18.2, 17.9, 17.7. IR (KBr, cm^{-1}): 3431, 3275, 3072, 2958, 2862, 1732, 1634, 1546, 1455, 1386, 1370, 1216, 1159.HRMS-ESI: m/z Calcd for $C_{41}H_{78}N_9O_8$ [M+H]$^+$ 824.5973, found: 824.5980.

4.2.5. [12]aneN$_3$–CH$_2$COLeuAlaLeuAlaLeuLeuOCH$_3$·3HCl 7e·3HCl

Yield, 87%. ^{1}H NMR (400 MHz, DMSO+D$_2$O) δ (ppm) 4.36–4.17 (m, 6H), 3.59 (s, 3H), 3.46 (s, 2H), 3.15–3.03 (m, 12H), 2.02 (s, br, 2H), 1.85 (s, br, 4H), 1.60–1.42 (m, 12H), 1.34–1.16 (m, 6H), 0.89–0.81 (m, 24H). ^{13}C NMR (101 MHz, DMSO) δ (ppm) 173.7, 172.7, 172.0, 171.9, 171.7, 171.6, 171.2, 54.9, 51.8, 50.6, 50.1, 48.0, 40.9, 40.8, 40.6, 24.2, 24.1, 24.0, 23.1, 22.8, 21.6, 21.5, 21.4, 21.3, 17.9. IR (KBr, cm^{-1}): 3418, 2959, 2872, 1732, 1635, 1548, 1455, 1386, 1365, 1271, 1119. HRMS-ESI: m/z Calcd for $C_{42}H_{80}N_9O_8$ [M+H]$^+$ 838.6130, found: 838.6133.

4.2.6. [12]aneN$_3$–CH$_2$COLeuAlaLeuAlaLeuPheOCH$_3$·3HCl 7f ·3HCl

Yield, 88%. ^{1}H NMR (400 MHz, DMSO+D$_2$O) δ (ppm) 7.27–7.17 (m, 5H), 4.45–4.41 (m, 1H), 4.35–4.19 (m, 5H), 3.62 (s, 3H), 3.55 (s, 2H), 3.15–2.88 (m, 12H), 2.03 (s, br, 2H), 1.88 (s, br, 4H), 1.60–1.34 (m, 9H), 1.20 (d, J = 7.0 Hz, 3H), 1.14 (d, J = 7.0 Hz, 3H), 0.88–0.78 (m, 18H). ^{13}C NMR (101 MHz, DMSO) δ (ppm) 171.9, 171.7, 171.5, 171.2, 137.1, 129.0, 128.1, 126.4, 54.8, 53.4, 51.8, 51.3, 48.1, 48.0, 40.9, 40.6, 36.5, 24.2, 24.0, 23.0, 22.9, 21.6, 21.5, 21.4, 17.8, 17.7. IR (KBr, cm^{-1}): 3422, 3066, 2958, 1735, 1643, 1541, 1456, 1386, 1369, 1222, 1167, 702. HRMS-ESI: m/z Calcd for $C_{45}H_{78}N_9O_8$ [M+H]$^+$ 872.5973, found: 872.5969.

4.2.7. [12]aneN$_3$–CH$_2$COLeuAlaLeuAlaLeuTyrOCH$_3$·3HCl 7g·3HCl

Yield, 83%. ^{1}H NMR (400 MHz, DMSO+D$_2$O) δ (ppm) 6.96 (d, J = 8.3 Hz, 2H), 6.64 (d, J = 8.3 Hz, 2H), 4.364–22(m, 6H), 3.54 (s, 5H), 3.15–3.03 (m, 12H), 2.90–2.78 (m, 2H), 2.03 (s, br, 2H), 1.84 (s, br, 4H), 1.59–1.35 (m, 9H), 1.20 (d, J = 7.0 Hz, 3H), 1.15 (d, J = 7.0 Hz, 3H), 0.88–0.79 (m, 18H). ^{13}C NMR (101 MHz, DMSO) δ (ppm) 171.9, 171.9, 171.8, 171.6, 171.5, 171.2, 156.0, 129.9, 126.9, 115.0, 54.9, 53.8, 53.8, 51.7, 51.7 51.3, 50.9, 50.7, 48.1, 47.9, 40.9, 40.8, 40.6, 35.8, 24.2, 24.0, 23.1, 23.0, 21.6, 21.6, 21.4, 17.9, 17.8. IR (KBr, cm^{-1}): 3278, 2957, 2871, 1742, 1650, 1538, 1512, 1451, 1387, 1369, 1217, 1170, 1053, 848, 753. HRMS-ESI: m/z Calcd for C45H78N9O9 [M+H]$^+$ 888.5923, found: 888.5940.

4.2.8. [12]aneN$_3$–CH$_2$COLeuAlaLeuAlaLeuTrpOCH$_3$·4HCl 7h ·4HCl

Yield, 87%. ^{1}H NMR (400 MHz, DMSO+D$_2$O) δ (ppm) 7.45 (d, J = 7.9 Hz, 1H), 7.33 (d, J = 8.0 Hz, 1H), 7.13 (s, 1H), 7.05 (t, J = 7.5 Hz, 1H), 6.97 (t, J = 7.4 Hz, 1H), 4.47 (t, J = 6.8 Hz, 1H), 4.36–4.23 (m, 5H), 3.52 (s, 3H), 3.47 (s, 2H), 3.16–3.04 (m, 14H), 2.02 (s, br, 2H), 1.86 (s, br, 4H), 1.61–1.51 (m, 4H), 1.47–1.40 (m, 5H), 1.20 (d, J = 7.1 Hz, 3H), 1.14 (d, J = 7.0 Hz, 3H), 0.88–0.80 (m, 18H).^{13}C NMR (101 MHz, DMSO) δ (ppm) 172.1, 172.0, 171.8, 171.7, 171.6, 171.3, 136.0, 127.1, 123.6, 121.0, 118.5, 118.0, 111.5, 109.2, 54.7, 53.4, 53.1, 51.9, 51.8, 51.3, 50.9, 48.0, 40.9, 40.8, 40.7, 26.9, 24.3, 24.1, 23.1, 21.7, 21.5, 17.8, 16.8. IR (KBr, cm^{-1}): 3276, 3060, 2956, 2928, 2871, 1729, 1694, 1629, 1541, 1454, 1387, 1369, 1215, 1165, 748, 708. HRMS-ESI: m/z Calcd for $C_{47}H_{79}N_{10}O_8$ [M+H]$^+$ 911.6082, found: 911.6072.

4.3. Agarose gel electrophoresis

Negatively supercoiled pUC18 DNA (0.4 μL, 450 μg/mL) was treated with each conjugate **7a–h** in Tris–HCl (2 μL, 50 mM, pH 7.4), followed by dilution with the water to a total volume of 20 μL. The samples were then incubated at 37 °C for 1 h. Then the loading buffer 2 μL (10 mM Tris–HCl, pH 7.6, 0.03% bromophenol blue, 0.03% xylene cyanol, 60% glycerol, 60 mM EDTA) was added to the mixtures. The solutions were analyzed by electrophoresis for 35 min at 70 V on a 1.0% agarose gel in 1 × TAE buffer. The gel was stained with Goldview II (1.0 μg/mL) and photographed on an UVP EC3 visible imaging system.

4.4. Dynamic light scattering

Dynamic laser light scattering (DLS) equipment was used to determine the average size of DNA nanoparticles condensed by different agents at 25 °C. The scattering angle was set to 90°. Typically, 10 runs were measured for each solution, with the average of all the runs reported. DNA solutions (9 μg/mL) were prepared

in the presence of each conjugate **7e**, **7f**, and **7h** (Tris buffer 50 mM, pH 7.4) with deionised Milli-Q water (18.25 MΩ). The mixture was allowed to stand for 5 min at room temperature and then 40 μL of the solution was transferred into the standard quartz cuvette for measurement.

4.5. Atomic force microscopy

A stock solution of pUC18 DNA (450 μg/mL) was diluted to 9 μg/mL (Tris buffer 5 mM, pH 7.4, $MgCl_2$ 1 mM) in the presence of each conjugate **7e**, **7f**, and **7h**. $MgCl_2$ were used optimally in order to facilitate the adhesion of DNA onto mica for better viewing. Then the corresponding solutions were left to equilibrate at 37 °C for 1 h. Subsequently, samples were studied by AFM in air condition. Freshly cleaved mica was used as substrate for all AFM imaging. Pretreatment of mica was necessary to promote electrostatic immobilization between the condensates and mica. Thus 15 μL of a 10 mM $NiCl_2$ solution was deposited for 2 min onto the surface of mica. The mica was then thoroughly rinsed with pure water to prevent the formation of salt crystals on the surface. A total of 10 μL of DNA solution was spotted onto the pretreated mica and incubated for 5 min. After which the mica was thoroughly rinsed with water and dried under a gentle steam of argon. AFM images were obtained in the air at room temperature with a Veeco atomic force microscope. Scan were run at a rate of 1–3 Hz operating in tapping mode using conical-shaped Si tips integrated to nano-crystalline Si cantilevers with an average resonance frequency of 280 kHz. The images were analyzed with the software accompanying with the imaging module.

4.6. EB displacement assay

A Cary Eclipse Luminescence Spectrometer was used for the EB displacement assay to confirm the DNA binding ability of the DNA condensing agents in Tris buffer (50 mM, pH 7.4) at room temperature. CT-DNA (100 μM) was first treated with EB (ethidium bromide, 10 μM), then the conjugate **7e**, **7f**, and **7h** was added, respectively. The mixture was incubated for 1 min prior to measurement (excitement wavelength 537 nm). The apparent binding constant (K_{app}) was calculated using the equation:[34,35]

$$K_{EB} \cdot [EB] = K_{app} \cdot [\text{condensing agent}]$$

where $K_{EB} = 1.0 \times 10^7\ M^{-1}$, [EB] = 10 μM, and [condensing agent] was the concentration at which a 50% reduction of the fluorescence had occurred.

4.7. Ionic strength effect

The influence of ionic strength on DNA condensation was investigated by agarose gel electrophoresis at 37 °C. pUC18 DNA (9 μg/mL) was treated with the condensing agents **7e**, **7f**, and **7h** in Tris buffer (50 mM, pH 7.4) in the presence of different concentrations of NaCl. After incubation for 1 h, the solutions were analyzed by electrophoresis as the method mentioned previously.

4.8. Release of the compact DNA

The reversibility of DNA condensation induced by the condensing agents was investigated by agarose gel electrophoresis at 37 °C in Tris buffer (50 mM, pH 7.4). pUC18 DNA (9 μg/mL) was first treated with the condensing agents (150 μM for **7e**, 250 μM for **7f**, and **7h**, respectively). After incubation for 1 h to facilitate the DNA condensation, the solutions were treated with NaCl at the concentrations of 50, 100, and 150 mM, respectively, then the mixtures were analyzed by electrophoresis as the method mentioned previously.

4.9. Cytotoxicity assay

The cytotoxicity of compound **7e**, **7f**, and **7h** toward HepG2 and T98G cell lines were tested by MTT assays (MTT = 3-(4, 5-dimethylthiazol-2-yl)-2, 5-diphenyltetrazolium bromide). HepG2 cells were cultured in Dulbecco's modified Eagle's medium (DMEM, Gibco) supplemented with fetal bovine serum (15%, v/v) and T98G cells were cultured in minimum essential medium (MEM, Gibco) supplemented with fetal bovine serum (10%, v/v) in a humid atmosphere containing 5% CO2 at 37 °C. After 48 h of incubation in the medium, the cells were seeded in 96-well plates at 5×10^5 cells per well and cultured for another 24 h. Then the cells were treated with different concentrations of **7e**, **7f**, and **7h** for 24 h, after which time the medium was removed and 10 μL of MTT (5 mg/mL) was added to wells along with 90 μL of culture medium. The cells were incubated for 4 h and the MTT containing medium was replaced with 110 μL of DMSO. Finally the plates were oscillated for 10 min to fully dissolve the formazan crystal formed by living cells in the wells. The absorbance of the purple formazan was recorded at 490 nm using a Bio-Rad 680 plate reader. The relative viability of the cells was calculated based on the data of four parallel tests by comparing to the controls.

Acknowledgments

The authors gratefully acknowledge the financial assistances from the Fundamental Research Funds for the Central Universities (2009SC-1); Beijing Municipal Commission of Education; Program for New Century Excellent Talents at Universities (NCET-08-0054), the Ministry of Education of China; and the Nature Science Foundation of China (20972019).

Supplementary data

Supplementary data associated with this article can be found, in the online version, at http://dx.doi.org/10.1016/j.bmc.2012.03.022.

References and notes

1. Tong, H. J.; Shi, Q.; Fernandes, J. C.; Liu, L.; Dai, K. R.; Zhang, X. L. *Curr. Gene Ther.* **2009**, *9*, 495.
2. Mintzer, M. A.; Simanek, E. E. *Chem. Rev.* **2009**, *109*, 259.
3. Itaka, K.; Kataoka, K. *Eur. J. Pharm. Biopharm.* **2009**, *71*, 475.
4. Collins, L. In *Methods in Molecular Biology*; Hornick, P., Rose, M., Eds.; Humana Press Inc, 2006; p 201.
5. Pelta, J.; Livolant, F.; Sikorav, J.-L. *J. Biol. Chem.* **1996**, *271*, 5656.
6. Jere, D.; Jiang, H. L.; Arote, R.; Kim, Y. K.; Choi, Y. J.; Cho, M. H.; Akaike, T.; Cho, C. S. *Expert Opin. Drug Deliv* **2009**, *6*, 827.
[7]. Xiang, Y. Z.; Wang, N.; Zhang, J.; Li, K.; Zhang, Z. W.; Lin, H. H.; Yu, X. Q. *Sci. China, Ser. B* **2009**, *52*, 483.
8. Liu, Y.; Yu, L.; Chen, Y.; Zhao, Y.-L.; Yang, H. *J. Am. Chem. Soc.* **2007**, *129*, 10656.
9. Bombelli, C.; Faggioli, F.; Luciani, P.; Mancini, G.; Sacco, M. G. *J. Med. Chem.* **2005**, *48*, 5378.
10. Felgner, P. L.; Gadek, T. R.; Holm, M.; Roman, R.; Chan, H. W.; Wenz, M.; Northrop, J. P.; Ringold, G. M.; Danielsen, M. *Proc. Natl. Acad. Sci. U.S.A.* **1987**, *84*, 7413.
11. Stamatatos, L.; Leventis, R.; Zuckermann, M. J.; Silvius, J. R. *Biochemistry* **1988**, *27*, 3917.
12. Saccardo, P.; Villaverde, A.; Gonzalez-Montalban, N. *Biotechnol. Adv.* **2009**, *27*, 432.
13. Lo, S. L.; Wang, S. *Biomaterials* **2008**, *29*, 2408.
14. Haley, J.; Kabiru, P.; Geng, Y. *Mol. Biosyst.* **2010**, *6*, 249.
15. Medina, S. H.; El-Sayed, M. E. H. *Chem. Rev.* **2009**, *109*, 3141.
16. Dong, X.; Wang, X.; He, Y.; Yu, Z.; Lin, M.; Zhang, C.; Wang, J.; Song, Y.; Zhang, Y.; Liu, Z.; Li, Y.; Guo, Z. *Chem. Eur. J.* **2010**, *16*, 14181.
17. Sun, B.; Guan, J.-X.; Xu, L.; Yu, B.-L.; Jiang, L.; Kou, J.-F.; Wang, L.; Ding, X.-D.; Chao, H.; Ji, L.-N. *Inorg. Chem.* **2009**, *48*, 4637.
18. Meng, X.-G.; Liu, L.; Zhou, C.-S.; Wang, L.; Liu, C.-L. *Inorg. Chem.* **2008**, *47*, 6572.
19. Gomez-Segura, J.; Prieto, M. J.; Font-Bardia, M.; Solans, X.; Moreno, V. *Inorg. Chem.* **2006**, *45*, 10031.
20. Zheng, J.; Li, Z.; Wu, A.; Zhou, H.; Bai, H.; Song, Y. *Biochem. Biophys. Res. Commun.* **2002**, *299*, 910.
21. Huang, Q.-D.; Chen, H.; Zhou, L.-H.; Huang, J.; Wu, J.; Yu, X.-Q. *Chem. Biol. Drug Des.* **2008**, *71*, 224.

22. Zhou, L.-H.; Yang, M.; Zhou, H.; Zhang, J.; Li, K.; Xiang, Y.-Z.; Wang, N.; Tian, Y.-F.; Yu, X.-Q. *Chem. Biol. Drug Des.* **2009**, *73*, 216.
23. Li, C.; Tian, H.; Rong, N.; Liu, K.; Liu, F.; Zhu, Y.; Qiao, R.; Jiang, Y. *Biomacromolecules* **2011**, *12*, 298.
24. Goparaju, G. N.; Satishchandran, C.; Gupta, P. K. *Int. J. Pharm.* **2009**, *369*, 162.
25. Eissenberg, D. *Ann. Rev. Biochem.* **1984**, *53*, 595.
26. Liu, L.; Zhang, H.; Meng, X.-G.; Yin, J.; Li, D.-F.; Liu, C.-L. *Biomaterials* **2010**, *31*, 1380.
27. Yan, H.; Li, Z.-F.; Guo, Z.-F.; Lu, Z.-L.; Wang, F.; Wu, L.-Z. *Bioorg. Med. Chem.* **2012**, *20*, 801.
28. Vijayanathan, V.; Thomas, T.; Thomas, T. J. *Biochemistry* **2002**, *41*, 14085.
29. Wang, J.-T.; Xia, Q.; Zheng, X.-H.; Chen, H.-Y.; Chao, H.; Mao, Z.-W.; Ji, L.-N. *Dalton Trans.* **2010**, *39*, 2128.
30. Nomura, A.; Sugiura, Y. *J. Am. Chem. Soc.* **2004**, *126*, 15374.
31. Makita, N.; Yoshikawa, K. *Biophys. Chem.* **2002**, *99*, 43.
32. You, Y.-Z.; Yu, Z.-Q.; Cui, M.-M.; Hong, C.-Y. *Angew. Chem., Int. Ed.* **2010**, *49*, 1099.
33. Li, C.; Tian, H.; Duan, S.; Liu, X.; Xu, P.; Qiao, R.; Zhao, Y. *J. Phys. Chem. B* **2011**, *115*, 13350.
34. Alkhader, S.; Ezra, A.; Kasparkova, J.; Brabec, V.; Yavin, E. *Bioconjugate Chem.* **2010**, *21*, 1425.
35. Dong, X.-D.; Wang, X.-Y.; Lin, M.-X.; Sun, H.; Yang, X.-L.; Guo, Z.-J. *Inorg. Chem.* **2010**, *49*, 2541.